EUROPHYSICS LETTERS 15 May 2003

Europhys. Lett., **62** (4), pp. 477–483 (2003)

Revealing the non-s^2 contributions in the momentum wave function of ground-state He

H. Schmidt-Böcking[1](*), V. Mergel[1], R. Dörner[1], C. L. Cocke[2], O. Jagutzki[1], L. Schmidt[1], Th. Weber[1], H. J. Lüdde[3], E. Weigold[4], J. Berakdar[5], H. Cederquist[6], H. T. Schmidt[6], R. Schuch[6] and A. S. Kheifets[4]

[1] *Institut für Kernphysik, Universität Frankfurt August-Euler-Str. 6, 60486 Frankfurt, Germany*

[2] *Department of Physics, Kansas State University - Manhattan, KA 66506, USA*

[3] *Institut für Theoretische Physik, Universität Frankfurt Robert-Mayer-Str. 6, 60487 Frankfurt, Germany*

[4] *RSPhysSE, Australian National University - Canberra 0200, Australia*

[5] *Max-Planck Institut für Mikrostruktur Physik - Weinberg 2, 06120 Halle, Germany*

[6] *Department of Physics, Stockholm University - S-10405 Stockholm, Sweden*

(received 4 October 2002; accepted in final form 20 March 2003)

PACS. 34.70.+e – Charge transfer.

PACS. 34.50.Fa – Electronic excitation and ionization of atoms (including beam-foil excitation and ionization).

PACS. 39.90.+d – Other instrumentation and techniques for atomic and molecular physics.

Abstract. – The correlated Tunneling Transfer Ionization (TuTI) channel in fast 4-body processes $p + He \rightarrow H^0 + He^{2+} + e$ is utilized to probe the highly correlated asymptotic parts of the He ground-state momentum space wave function. In this reaction, predominantly at large nuclear impact parameters, one electron in the He ground state is captured by the proton by tunneling through the two-center barrier when electron and proton velocity vectors resonantly match. The measured 3-particle final-state momentum distributions show characteristic features that we trace back to the highly correlated non-s^2 components of the He ground-state momentum wave function. This conclusion is supported by a simple heuristic model.

In atomic physics, the ground state of He provides an ideal test case for studying the correlated motion of electrons in a bound few-electron system [1]. In this paper we reveal new information on the electron correlation in He by employing a novel high-resolution momentum imaging technique. A very small fraction of the He ground-state occupation probability is projected onto the continuum by an electron capture reaction in which one electron is picked up by a fast proton and the second electron is left in the continuum. The correlation can be seen directly in the momentum distribution of the continuum electron rather than having to be deduced indirectly from measured cross-section ratios. The momentum vectors of the two

(*) E-mail: schmidtb@ikf.uni-frankfurt.de

electrons and the nucleus in the initial state are determined in a very sudden fragmentation process which takes a nearly unperturbed snapshot of the highly correlated three-particle motion in the He ground state. We argue that this fragmentation process proceeds most likely via the non-s^2 components of the He ground state. These components make up only a very small fraction ($< 10^{-2}$) of the He ground state [2,3] and are therefore difficult to probe with standard techniques such as spectroscopy. Nevertheless, these small fractions might be of fundamental importance for the interaction of He with its environment [4,5].

In the study presented here we choose a specific channel of the electron capture by a fast proton —the correlated Tunneling Transfer Ionization (TuTI) [6,7]. In the TuTI process, one electron (labelled 1 for definiteness) is captured by a fast proton by tunneling through the two-center barrier when the electron and proton velocity vectors match (a Brinkman-Kramers–type capture) nearly exclusively to the H^0 $1s$ state and the second electron (labelled 2) is simultaneously ejected into the continuum. In the TuTI channel the proton transfers energy, but only a small amount of momentum to the He atom, both quantities being determined experimentally. We also measure all the transverse momenta in the final state and therefore have qualitative information on the nuclear impact parameter. We can then distinguish between close and distant nuclear collisions. The perturbation of the correlated momentum wave function of He by the proton is negligible in comparison with the large initial momentum vectors of the two electrons. The initial velocity of the captured electron always exceeds the mean velocity of an electron in the He ground state. Thus, in momentum space, electron 1 is captured from the asymptotic part of the He ground state.

Since the force of the fast departing neutral H^0 on the remaining He^+ decreases rapidly, the final-state interaction between H^0 and the fragments is negligibly small. We can also rule out ejection of the second electron via subsequent interaction of the projectile with the target [6]. Rather, this ejection is expected to be due to a shake-off process in which a sudden removal of electron 1 from the highly correlated initial state leaves electron 2 in the continuum. Should electron 1 be captured from the non-s^2 components of the ground state [8,9], the probability for ejecting electron 2 would be close to 100%. A non-s^2 electron cannot remain in the He $1s$ ground state because of angular momentum conservation. At these fast proton velocities also excitation of electron 2 to higher He states is rather small [7].

The TuTI process competes with other transfer ionization (TI) channels [6–8,10–16]. Each channel can be identified by a characteristic pattern in the H^0 and He^{2+} final-state momentum phase space. This is achieved by measuring, in coincidence, the 5 final-state momentum components (3 of the He^{2+} recoil momentum and 2 of the H^0 transverse momentum). An extremely high resolution (better than 10^{-5} of the projectile momentum, equivalent to 100 μeV in recoil-ion energy) is required. Further, a very high detection efficiency is needed as the TuTI cross-section is typically only of the order of barns.

We have carried out these measurements using the high momentum resolution and multi-coincidence efficiency of COLd Target Recoil Ion Momentum Spectroscopy (COLTRIMS) [17]. The complete final-state momentum distributions for fast TI processes (proton energy $E_\mathrm{p} =$ 0.15 to 1.4 MeV) were measured at the 2.5 MeV Van de Graaf accelerator of the Institut für Kernphysik of the Universität Frankfurt. Details of the experiment are given in ref. [7].

Different scattering regimes can be identified by analyzing the TI cross-section as a function of the H^0 transverse momentum $k_{x,\mathrm{H^0}} = M_\mathrm{p} v_\mathrm{p} \theta_{\mathrm{H^0}}$, where $\theta_{\mathrm{H^0}}$ is the deflection angle of the hydrogen atom. The longitudinal z component of the H^0 momentum is defined along the beam direction and the y component (in direction perpendicular to the H^0 scattering plane) is set to zero for each scattering event. The TI cross-sections differential with respect to $k_{x,\mathrm{H^0}}$ at varying proton energies $E_\mathrm{p} = 0.15$–1.4 MeV were analyzed by Mergel *et al.* [6,7]. At small deflection angles $\theta_{\mathrm{H^0}} < 0.6$ mrad, the TI cross-sections showed a characteristic "hump"

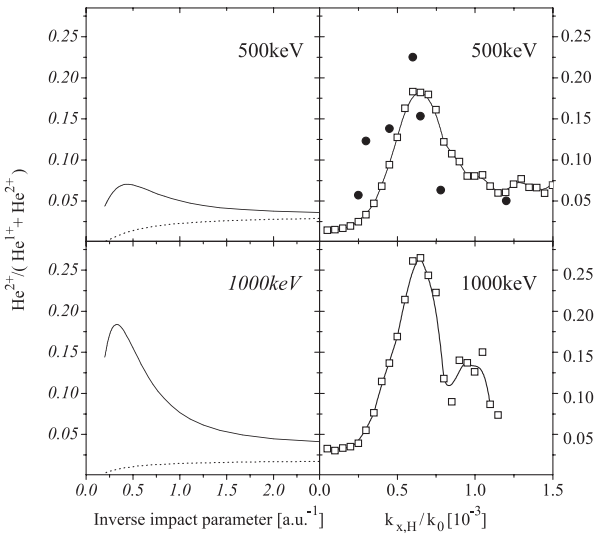

Fig. 1 – Right panel: experimental ratio of TI to single-capture cross-sections differential in θ_{H^0} for 500 and 1000 keV proton impact energy (open circles: data of [7], solid circles: data of Giese *et al.* [11]; solid line: fit to the data). Left panel: calculations of Kheifets [9]; dotted lines: s^2 components, solid lines: including non-s^2 components (see the text).

which was even more pronounced on the differential cross-sections of the single capture (SC) process in which the second electron remained bound. Mergel *et al.* [6] identified this "hump" region with distant nuclear collisions (large nuclear impact parameters) in which the proton is deflected only by the initial transverse momentum of the captured electron. At larger values of k_{x,H^0}, where the slope of the SC curves becomes less steep, the transverse momentum exchange is largely between the projectile and the He nucleus (small nuclear impact parameters).

In the plot of the ratio of TI to single capture cross-sections differential in θ_{H^0} (fig. 1, right panel), the same puzzling peak was observed at about 0.65 mrad [7], as in the experiment of Giese *et al.* [11]. Measuring the longitudinal energy loss of the projectile with high precision, Mergel *et al.* [6, 7] also showed that this peak cannot be explained by any of the known TI processes.

In fig. 1, for 500 and 1000 keV proton impact energy, the experimental ratios (right panel) are shown in comparison with theoretical predictions of Kheifets [9] (left panel), where the influence of different angular momentum components in the ground-state wave function is investigated.

This calculation is based on the following simple heuristic model, since no rigorous quantum-mechanical theory has been put forward so far to explain the present experiment. We assume that the angular distribution of the transfer ionized and ejected electrons is governed by the projection of the He atom ground state onto the two-electron continuum:

$$\langle \boldsymbol{k}_1 \boldsymbol{k}_2 \mid \Phi_0 \rangle = \sum_{nl} A_{nl} C^{00}_{lm,l-m} \langle \boldsymbol{k}_1 \mid nlm \rangle \langle \boldsymbol{k}_2 \mid nl-m \rangle, \tag{1}$$

where z is the incident direction and x is the scattering direction. Here the Clebsch-Gordan coefficient $C^{00}_{lm,l-m}$ couples the two individual electron angular momenta to the $^1S_0$ ground state. The configuration interaction coefficients are found from the multi-configuration Hartree-Fock expansion and decrease rapidly with increasing n, l, the leading terms being $A_{1s} = 0.996$,

$A_{2s} = -0.059$, $A_{2p} = 0.059$, $A_{3d} = -0.012$. We assume that electron 1 is picked up by the proton at a finite distance in the transverse direction from the He nucleus of the order of the nuclear impact parameter, and write

$$\langle \boldsymbol{k}_1 \mid nlm \rangle \propto \int_a^\infty \mathrm{d}x e^{ik_x x} \int_{-\infty}^{\infty} \mathrm{d}z e^{ik_z z} R_{nl}(r) \exp[im\phi]. \tag{2}$$

Here we choose the angular momentum quantization axis in the y-direction and write the electron wave function in the scattering plane as $\phi_{nlm}(\boldsymbol{r}) = R_{nl}(r) Y_{lm}(\theta = \pi/2, \phi) \propto R_{nl}(r) \cdot \exp[im\phi]$, $\tan\phi = x/z$. In the second overlap $\langle \boldsymbol{k}_2 \mid nl - m \rangle$ the integration is expanded over the whole scattering plane and the final state $\langle \boldsymbol{k}_2 |$ is treated as the Coulomb wave in the field of the He^{2+} ion.

In a standard shake-off theory (see, *e.g.*, Shi and Lin [18]) the x integration in eq. (2) is expanded over the whole scattering plane and the integral becomes symmetric with respect to the sign reversal of the angular momentum projection m. In our model, due to restriction to $x > a$, there is a very large asymmetry between $\pm m$ components $P_{nlm}/P_{nl-m} \sim k_{1z}a \gg 1$. This asymmetry can be understood if one recalls that the departing electron carries away the angular momentum $k_z a$ and the projection of this momentum on the quantization axis favors only one particular sign of m. The large angular momentum $k_z a \gg 1$ has to be drawn from a ground-state orbital with a limited l, m. This makes the overlap integral exponentially small, $P_{nlm} \sim \exp[-k_z a]$. This smallness is offset by the growing power term $(\beta a)^l$, where β is the exponential fall-off parameter of the radial orbital R_{nl}. The power term compensates the small coefficients A_{nl} for $l > 0$. As a result, the strongest contribution to the amplitude of eq. (1) comes from the $2p_{+1}$ and $3d_{+2}$ terms but not the $1s$ one (see Kheifets [9] for more details).

Results of our calculation for $E_\mathrm{p} = 0.5$ and $1.0\,\mathrm{MeV}$ and varying inverse impact parameters are presented in the left panel of fig. 1. The calculations for pure s^2 components (dotted lines) show a smooth increase towards small impact parameters in clear disagreement with the data, whereas the calculations with inclusion of the non-s^2 components reproduce qualitatively the observed peak at small inverse (*i.e.* large) nuclear impact parameters. They even predict at large impact parameters shake-off ratios above 10%.

The abscissa in the left and right panels of fig. 1 cannot directly be compared, but from the data in refs. [6, 7] we can estimate the nuclear impact parameter in the regime of very small projectile scattering angles. Using this width we get for the very small θ_{H^0} a lower limit for the nuclear impact parameter $a \gtrsim 1.2$ and $0.6\,\mathrm{a.u.}$ for $E_\mathrm{p} = 0.5$ and $1\,\mathrm{MeV}$, respectively.

Fully differential cross-sections projected on the projectile scattering plane, *i.e.* measured momentum distributions of electron 2, are shown in fig. 2 at the proton energy $E_\mathrm{p} = 0.3\,\mathrm{MeV}$ and different deflection angles [6]. At very small deflection angles, besides the puzzling peak in fig. 1, more surprising features of the measured momentum patterns can be seen:

i) Electron 1, the He^{2+} ion (see [6]) and electron 2 always share comparable momenta. None of these particles in the Lab system final state shows a momentum distribution peaking at zero. If electron 2 were a slow electron ejected in an s-wave shake-off process, the recoil momentum would be expected to peak near $\boldsymbol{k}_\mathrm{r} = (0, 0, -\frac{1}{2} v_{\mathrm{H}^0})$ and the corresponding electron momentum distribution would peak at the origin.

ii) The momentum vector distribution of the He^{2+} ion, and therefore that of electron 2, always peak in the H^0 scattering plane.

iii) Electron 2 is predominantly emitted into the backward and opposite direction, *i.e.* its emission is very asymmetric with respect to the scattered projectile and electron 1.

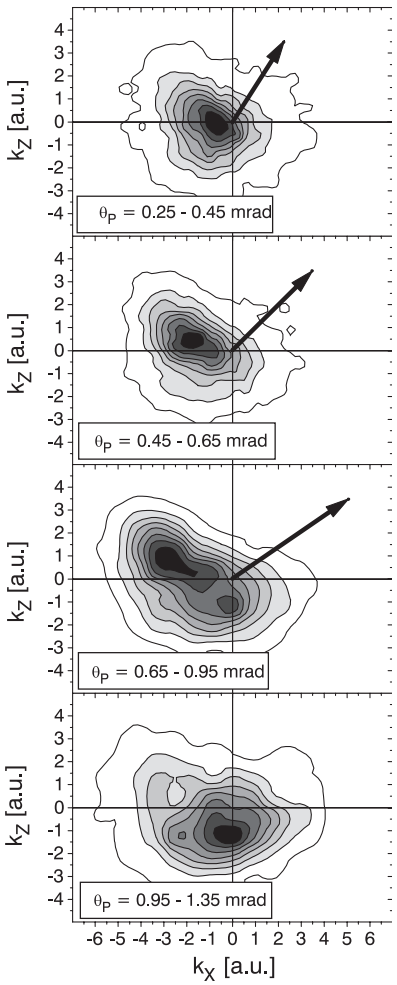

Fig. 2

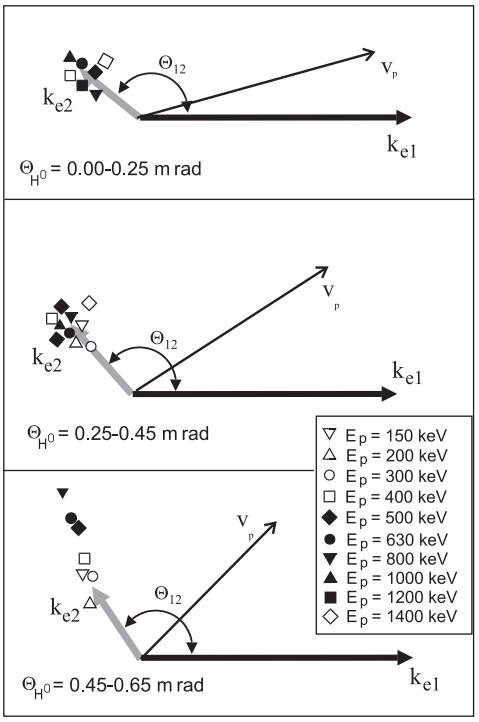

Fig. 3

Fig. 2 – Experimental momentum distributions of electron 2 projected on the H^0 scattering plane at $E_p = 0.3$ MeV and various proton deflection angles ($\theta_{H^0} = 0.25$–0.45, 0.45–0.65, 0.65–0.95 and 0.95–1.35 mrad). The black vectors indicate the mean location of $\boldsymbol{k}_1$ as deduced from eq. (3).

Fig. 3 – Initial-state momentum relation between the two electrons in the He ground state derived from the data (see text) for different impact energies E_p and three angles θ_{H^0}. The vector v_p indicates the direction of the impacting proton, the vectors $\boldsymbol{k}_1$ and $\boldsymbol{k}_2$ those of the electrons.

In ref. [6] it is shown in detail that these experimental findings cannot be explained by any of the so far known TI reaction mechanisms and by existing shake-off theories.

However, the here presented calculations for non-s^2 components [9] reproduce ii): the coplanar emission of electron 2 and recoil ion in the projectile scattering plane, and iii), that the angular distribution of electron 2 is very anisotropic at large a due to significant contributions from the non-s^2 components of the ground state.

Furthermore, the here presented calculations predict that the non-s^2 components yield the dominant contribution to the total TuTI cross-section in agreement with our data. From

our experimentally derived fully differential cross-sections we estimate that at 1 MeV impact energy the relative contributions to the total TI cross-sections are: more than 75% non-s^2 TuTI, less than 5% s^2 TTI, and about 20% e-e TTI (*i.e.* the classical billiard-like Thomas Transfer Ionization process [19]).

But observation i) is in clear contradiction to the calculations. For both the s^2 as well the non-s^2 components the calculations predict electron 2 momentum peaking at or near zero.

To shed more light on the dynamical correlation of the non-s^2 components in the He ground state, the initial electron momenta can be deduced from the measured final-state momentum distributions in the distant nuclear collision regime ($\theta_{\mathrm{H}^0} < 0.6\,\mathrm{mrad}$). Indeed, electron 1 can only be captured by the proton if its initial-state wave function in momentum space overlaps with the Compton profile of the hydrogen atom. The maximum of this overlap in the longitudinal direction lies between $\frac{1}{2}v_{\mathrm{H}^0}$ and v_{H^0}. For simplicity, we ignore the Compton spread of the captured electron and use the value v_{H^0} for the longitudinal matching condition. As to the transverse momentum received by the H^0 projectile, it is delivered by, and therefore identical to, that of electron 1 in the initial state. Thus the incident projectile picks up electrons with initial-state momentum vector,

$$\boldsymbol{k}_1 = \big(k_x = k_{x\mathrm{H}^0}, k_y = 0, k_z = v_{\mathrm{H}^0}\big). \tag{3}$$

In the laboratory frame the mean value of the momentum vector of the ejected electron $\boldsymbol{k}_2$ varies strongly with E_{p} and θ_{H^0}. If, however, we plot the most likely value of $\boldsymbol{k}_2$ with respect to $\boldsymbol{k}_1$ (derived from eq. (3) and indicated as black arrows in fig. 2), the momentum pattern becomes almost independent of the projectile velocity and deflection angle. This pattern is presented in fig. 3 for all the investigated impact energies E_{p} at three very small angles θ_{H^0}. Here $\boldsymbol{k}_1$ is always plotted to the right and normalized to 1, while $\boldsymbol{k}_2$ is scaled accordingly in its length. The angle between the electrons (counted in the direction opposite to θ_{H^0}) appears nearly constant with $\theta_{12} = -140^\circ \pm 25^\circ$. The ratios of the magnitudes of the momenta are constant within the experimental uncertainty of about $\pm 20\%$. It is striking to see that the TuTI process always yields a similar momentum pattern.

We conclude that peculiarities of the TuTI process, first observed by Mergel *et al.* [6] and further analyzed in the present work, can be explained by the contributions of non-s^2 components in the He ground-state wave function to the TuTI process. Thus, the virtually excited non-s^2 components can be revealed by the imaging techniques applied here.

Our simple model [9] describes most of the main features of the experimental data, the coplanar emission of recoil ion and electron 2 in the hydrogen scattering plane, and the asymmetric emission of electron 2. It clearly demonstrates that the dominant contributions to TuTI result from distant nuclear collision regimes. However, the model is so far too crude to reproduce all the details of the experiment. In particular the large momenta of electron 2 at small H^0 scattering angles cannot yet be reproduced as well as the scaling of the emission pattern shown in fig. 3.

* * *

We acknowledge numerous fruitful disputes and discussions with our colleagues and friends. In particular, Yu. Popov has challenged us on many occasions. VM acknowledges the support by the Studienstiftung des Deutschen Volkes and EW the support by the Humboldt-Stiftung. This work was supported by the DFG, the BMBF, GSI-Darmstadt, Graduiertenprogramm des Landes Hessen, and Röntdek GmbH.

REFERENCES

[1] Tanner G., Richter K. and Rost J.-M., *Rev. Mod. Phys.*, **72** (2000) 497.
[2] Kinoshita T., *Phys. Rev.*, **115** (1959) 366.
[3] Drake G. W. F., in *Long Range Casimir Forces*, edited by Levin F. S. and Micha D. A. (Plenum, New York) 1994, p. 107.
[4] Efimov V. M., *Commun. Nucl. Part. Phys.*, **19** (1990) 271.
[5] Macek J., *Z. Phys. D*, **3** (1986) 31.
[6] Mergel V., Dörner R., Khayyat K., Achler M., Weber T., Jagutzki O., Lüdde H. J., Cocke C. L. and Schmidt-Böcking H., *Phys. Rev. Lett.*, **86** (2001) 2257.
[7] Mergel V., PhD Thesis, University of Frankfurt (1996).
[8] Schmidt-Böcking H. *et al.*, in *AIP Conf. Proc.*, edited by Madison D. and Schulz M., Vol. **604** (AIP) 2002, pp. 120-127.
[9] Schmidt-Böcking H., Kheifets A. S. *et al.*, in *Springer Series on Atomic, Optical, and Plasma Physics*, edited by Shevelko V. P. and Ullrich J., Vol. **35** (Springer, Heidelberg) 2003.
[10] Briggs J. S. and Taulbjerg K., *J. Phys. B*, **12** (1979) 2565.
[11] Giese J. P. and Horsdal E., *Phys. Rev. Lett.*, **60** (1988) 2018.
[12] Pálinkás J., Schuch R., Cederquist H. and Gustafsson O., *Phys. Rev. Lett.*, **63** (1989) 2464.
[13] Ishihara T. and McGuire J. H., *Phys. Rev. A*, **38** (1988) 3310.
[14] Schmidt H. T. *et al.*, *Phys. Rev. Lett.*, **89** (2002) 163201.
[15] McGuire J. H., Straton J. C. and Axmann W. J., *Phys. Rev. Lett.*, **62** (1989) 2933.
[16] McGuire J., Berrah N., Bartlett R., Samson J., Tanis J., Cocke C. and Schlachter A., *J. Phys. B*, **28** (1995) 913.
[17] Dörner R., Mergel V., Jagutzki O., Spielberger L., Ullrich J., Moshammer R. and Schmidt-Böcking H., *Phys. Rep.*, **330** (2000) 96.
[18] Shi T. Y. and Lin C. D., *Phys. Rev. Lett.*, **89** (2002) 163202.
[19] Thomas L. H., *Proc. R. Soc.*, **114** (1927) 561.